DIRECT NUMERICAL SIMULATION OF TURBULENT FLOW PAST HEXAGONAL CYLINDERS

Hatef A.Khaledi
Department of Energy and Process Engineering
NTNU
Trondheim, Norway
hatef.khaledi@ntnu.no

Helge I.Andersson
Department of Energy and Process Engineering
NTNU
Trondheim, Norway
Helge.i.andersson@ntnu.no

ABSTRACT

The unsteady wake behind a hexagonal cylinder in cross-flow is investigated numerically. The time-dependent three-dimensional Navier-Stokes equations are solved for moderately high Reynolds numbers Re and for two different cylinder orientations. The topology of the vortex shedding depends on the orientation and the Strouhal frequency is generally higher in the wake of a face-oriented cylinder than behind a corner-oriented cylinder. This behaviour is contradictory to earlier findings for square cylinder wakes.

INTRODUCTION

Since the early vortex study by Gerrard (1966) back to more than forty years ago that opened a way of understanding the near wake vortex formation, there had been numerous experimental and numerical investigations on wake dynamics mainly on the cylinder. This geometry has been the focus of many studies mostly due to their geometrical simplicity and their regular presence and practical relevance in industrial and engineering applications. The huge and overwhelming study of this kind has led to perceiving and describing the 2D and 3D vortex shedding process behind circular cylinders (Zdravkovich, 2003; Williamson, 1996). Although the cylinder with circular cross section has been the focus of most studies during the decades, but cylinders with other cross sections have been spotted albeit rather scarcely. Among them the flow around square cylinder has received some attention. Experimental results concerning pressure forces and lift and drag quantities have been available since the very first experiment performed by Vickery (1966). However new simulations try to generate the experimental results of Lyn and Rodi (1994) which has been performed at Re= 22000. Lyn and Rodi by means of laser-Doppler velocimetry analysed the turbulent shear layer and the recirculation region formed after a square cylinder. In another study, Lyn et al. (1995) obtained ensemble-averaged statistics at constant phase of the turbulent flow around a square cylinder and they differentiated the length and velocity scales and vortex properties between the flow around circular and square cylinder. In another experimental probe Bosch and Guterres (2001) studied the effect of wind on tapered cylinders. The project was aimed to understand the vortex induced vibration of highway support structures. For this purpose they made several tapered cylinders with different cross sections. The models were fabricated with circular, octagonal or hexagonal cross sections. However, in their report they only presented the results for circular and octagonal cross sections and the results concerning the wake behind hexagonal cylinder were not demonstrated.

Sohankar et al. (1997) simulated the unsteady 2D laminar flow around a square cylinder at various angles of attack. They calculated several quantities such as Strouhal number, drag and lift. They extended their work and publish another article (1998) on the study of blockage, onset of vortex shedding and the effect of boundary condition for this case.

In an attempt to seek for definitive information for surface-averaged Nusselt number for all standard circular and non-circular cylinders subjected to air flow, Sparrow et al. (2004) distilled a new set of correlations for heat transfer quantities. A group of non-circular cross-sections including the square, diamond, ellipse and hexagon were studied. Although the investigation has almost nothing to do with vortex dynamics and wake flow analysis over non-circular cylinders, one can find an analogy between variation of Nusselt number and Strouhal number in different cross-sections.

As mentioned earlier the hexagonal cylinder has not been the centre of attention. Therefore the aim of this study is to explore the physics of the wake flow behind a hexagonal cylinder. The study is based on fully resolved three-dimensional computer simulations, i.e. direct numerical simulations. The study is aimed to consider three different flow regimes: laminar, transition and turbulent flow. At turbulent flow the wake is undoubtedly unsteady and the separated flow is expected to become turbulent already in the near-wake. This investigation at different flow regimes is focused on wake topology and vortex dynamics. However, the averaged flow field and frequency analysis will also be presented and compared with the wake behind a square cylinder.

FLOW FIELD AND COMPUTATIONAL APPROACH

The flow over regular hexagons will be considered. Regular hexagon has all sides of the same length and all angels are 120°. Two different orientations have been simulated in this study. The first orientation called corner-oriented throughout the article meet the rightward inflow velocity with its left farmost edge. The other orientation (face-oriented) is rotated 60° and its most left side obstruct the incoming rightward flow perpendicularly. The centre of hexagon is positioned $5d_1$ downstream of the inflow plane where d_1 is the diameter of the circle in which the hexagons are inscribed and d_2 is the height of the hexagon when it sits on one side. The ratio $d_2/d_1 = 0.866$. The geometries are shown in Figure 1.

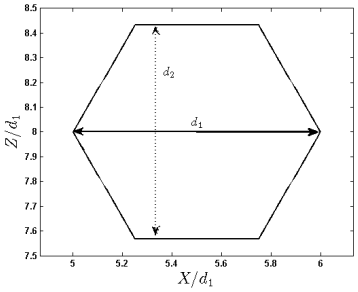

(a)

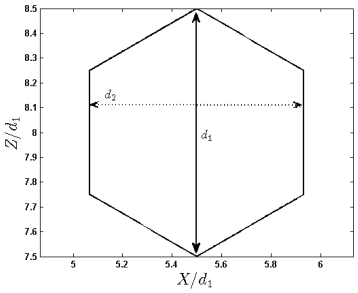

(b)

Figure 1. (a) Corner orinetation, (b) Face orinetation

Reynolds number $Re=U_0d_1/\nu$ based on uniform inflow velocity U_0 and the diameter d_1 is 1000. The flow field is conventionally described in a Cartesian coordinate system with the x-axis in the direction of inflow, the y-axis in spanwise direction and the z-axis directed across the flow. The size of computational domain in each coordinate direction is $L_x= 20d_1$, $L_y=6\ d_1$, and $L_z =16\ d_1$.

Face	Boundary Condition
Inflow	$U_0 = 1;\ V_0 = W_0 = 0;$ $\partial P/\partial x = 0$
Top & Bottom wall	$W = 0;$ $\partial U/\partial Z = \partial V/\partial Z = \partial P/\partial Z = 0$
Outflow	$P = 0;$ $\partial U/\partial X = \partial V/\partial X = \partial W/\partial X = 0$
Side Walls	Periodic

Table 1 Boundary conditions

Table 1 gives an overview of the boundary conditions used. A uniform velocity profile has been prescribed as inlet boundary condition. A Neumann boundary condition is set for pressure at the inflow and a free-slip condition was applied at top wall and bottom wall. Spanwise homogeneity enables us to use a periodic boundary condition at the side walls. At the outlet the Neumann and Dirichlet boundary condition were chosen for velocities and pressure, respectively.

The simulation has been performed by well-defined finite volume solver MGLET (Manhart, 2004) which has been tested and verified in several other cases. The three dimensional incompressible Navier-Stokes equations have been approximated on a staggered Cartesian grid system. Space derivatives were 2nd order accurate central-difference scheme and a 3rd order Runge-Kutta scheme was used for time advancement. The Poisson equation related to pressure field was calculated by using iterative Strongly Implicit Procedure (SIP). The Time stepping for all simulations equals to $\Delta t = 0.001 d_1/U_0$ and number of Poisson iterations per time was limited to 30. The the number of grid points is Nx=668, N_y= 80 and N_z= 400. Perhaps it is not needed to mention that the grids are denser around the body.

RESULTS AND DISCUSSIONS

In this section the vortex structure behind the hexagonal cylinders is visualized by means of instantaneous spanwise vorticity contours (ω_y) . The iso-surface of ω_y at time $t=100d/U_0$ for face-orientation is shown in Figure 2 whereas the vortex structure behind in the wake of corner-orientatio is depicted in Figure 3. Note that black contours are negative and white contours are positive.

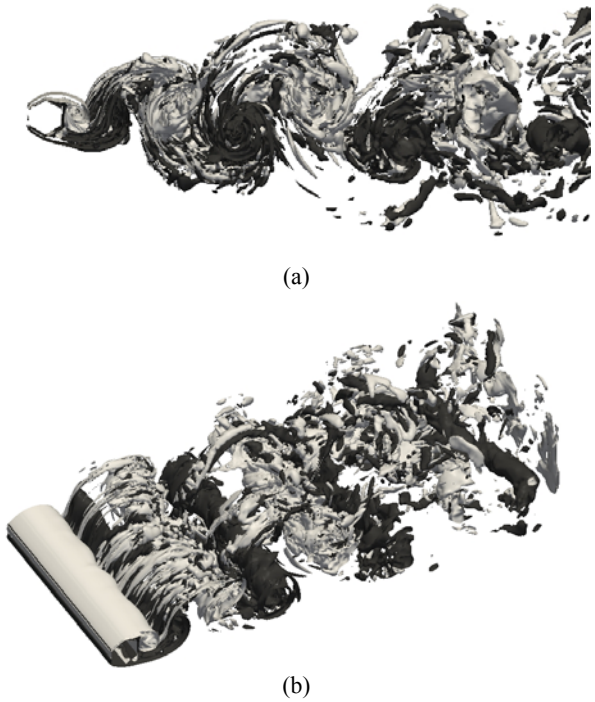

(a)

(b)

Figure 2 The Iso-surface of ω_y at time $t=100d_1/U_0$, Face-orientation (a) side view (b) Isometric view

The vorticity patterns in Figure 2 and 3 show that the spanwise-oriented Karman-like roller eddies are blurred by a highly irregular flow pattern downstream of the hexagon. The small disturbed vortex structures mimic the characteristics of turbulent flows. The irregularities arise in the shear layer along the flow-parallel hexagon. The longitudinal vortex filaments are stretched between two consecutive rollers. The vortex structures comparison between edge orientation and face orientation does not show much differences downstream.

The iso-contour plots of spanwise vorticity for the face orientation at Re=1000 (Figure 2a) shows that the flow separates from two edeges belong to the front surface. In the very near wake at Re=1000 the flow is mostly dominated by a big counter-clockwise roller (white) which has formed a laminar unsteady shear layer down to $1d_1$ downstream of the hexagon. However the disturbed and irregular pattern downstream of the hexagon shows that the shedding rollers eventually break into turbulent small structures. Figure 3a and 3b show the iso-contour plots of the corner orientation case at Re=1000.

The flow seems to separate somewhere along the flow-parallel faces rather than at the backward-facing corners or vertices. Vorticity field is destabilized already along the flow-parallel faces and the vortices are irregular from their detachment. The spanwise-oriented vortex cells can still be discerned, but the alternating positive and negative vorticity is blurred by smaller-scale irregularities.

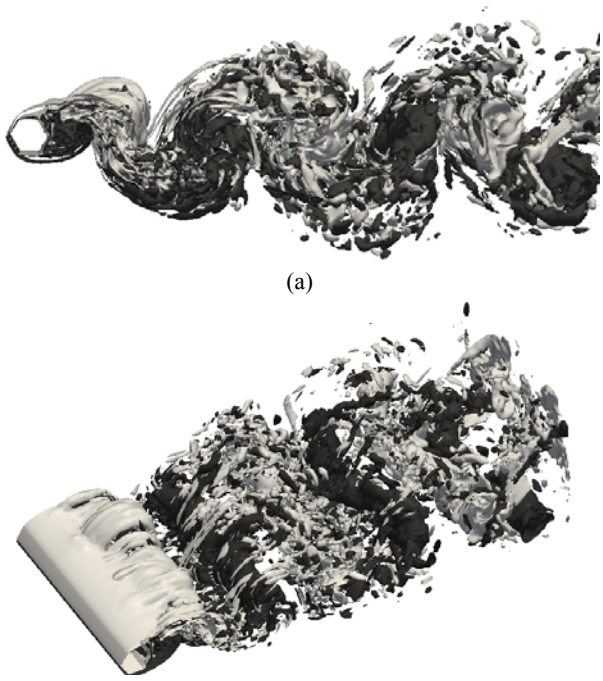

(a)

(b)

Figure 3 The Iso-surface of ω_y at time $t=100d_1/U_0$, Corner-orientation (a) side view (b) Isometric view

Let us start with the mean streamline plot after the hexagon. The mean streamline plot for face-orientation and corner-orientation hexagon is shown in Figure 4 (a) and (b) respectively.

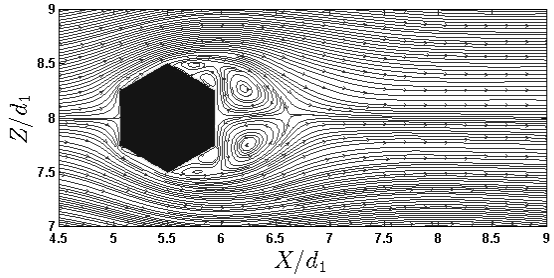

(a)

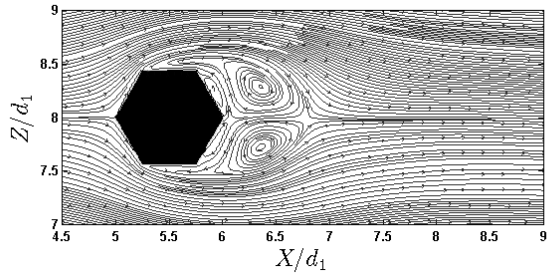

(b)

Figure 4 Mean streamline, Re=1000,(a) Face-orientation (b) Corner-orientation

The plots clearly visualize two big counter rotating bubbles after the body. In case of face orientation geometry these circulating bubbles are extended to X/d_1=6.645 whereas in corner orientation the bubbles are stretched to X/d_1=6.818. At this position the saddle point where the streamlines meet and the streamwise velocity changes sign, is detectable. In face-orientation hexagon, beside these two major circulating bubbles, there are two small pairs of counter –rotating bubbles behind the oblique sides of the hexagon. These pairs are probably driven by the two major bubbles and counter-interaction of one small rotating bubble on its own vicinity. On the other hand on the oblique sides of corner-orientation geometry two distinct bubbles that rotate in opposite directions of the major circulating bubbles are visible. In the case of corner-orientation the separation occurs in the very beginning of the upper wall. The backward velocity can be seen on the entire region over the upper side of the hexagon. The separation over the entire top edge is similar to the shear layer separating from the edge of square cylinder observed by Lyn & Rodi (1994)

REFERENCES

Bosch, H.R. and Guterres, R.M. 2001 "Wind tunnel experimental investigation on tapered cylinders for highway support structures," J. Wind Eng. Ind. Aerodyn. **89**, 1311

Gerrard, J.H. 1966. "The mechanics of the formation region of vortices behind bluff bodies" J Fluid Mech 25:401–413

Lyn, D. A., Einav, S., Rodi, W. AND Park, J. H. 1995. " A laser-Doppler velocimetry study of ensemble-averaged characteristics of the turbulent near wake of a square cylinder," *J . Fluid Mech.* 304, 285-315

Lyn, D. A. and Rodi,W. 1994 "The flapping shear layer formed by flow separation from the forward corner of a square cylinder," *J . Fluid Mech. 26, 353-376*

Manhart, M., 2004. "A zonal grid algorithm for DNS of turbulent boundary layers. " Computers & Fluids 33, 435–461.

Sohankar,A., Norberg, L., Davidson, L.1997, "Numerical simulation of unsteady low-Reynolds number flow around rectangular cylinder at incidence", Journal of Wind Engineering and Industrial Aerodynamics 69-71, 189-201

Sohankar,A., Norberg, L., Davidson,L. 1998," Low-Reynolds number flow around a square cylinder: study of blockage, onset of vortex shedding and outlet boundary condition" International Journal of Numerical Methods Fluids, 26,39-56

Sparrow, E. M. , Abraham, J. P. and Tong, J. C.K. 2004. " Archival correlations for average heat transfer coefficients for non-circular and circular cylinders and for spheres in cross-flow", Int. J. Heat and Mass Transfer. 47, 5285-5296

Williamson, C.H.K. 1996. "Vortex dynamics in the cylinder wake." Annu. Rev. Fluid Mech. 28, 477-539.

Zdravkovich, M.M. "Flow around Circular Cylinders. Vol. 1: Fundamentals. Vol. 2: Applications", Oxford Scientific Publisher, 1997, 2003.